BIOCHEMISTRY
including biophysical chemistry & molecular biology

Article

pubs.acs.org/biochemistry

Timing of Electron and Proton Transfer in the ba_3 Cytochrome *c* Oxidase from *Thermus thermophilus*

Christoph von Ballmoos,[†] Peter Lachmann,[†] Robert B. Gennis,[‡] Pia Ädelroth,[†] and Peter Brzezinski*[,†]

[†]Department of Biochemistry and Biophysics, The Arrhenius Laboratories for Natural Sciences, Stockholm University, SE-106 91 Stockholm, Sweden

[‡]Department of Biochemistry, University of Illinois, Urbana, Illinois 61801, United States

Supporting Information

ABSTRACT: Heme-copper oxidases are membrane-bound proteins that catalyze the reduction of O_2 to H_2O, a highly exergonic reaction. Part of the free energy of this reaction is used for pumping of protons across the membrane. The ba_3 oxidase from *Thermus thermophilus* presumably uses a single proton pathway for the transfer of substrate protons used during O_2 reduction as well as for the transfer of the protons that are pumped across the membrane. The pumping stoichiometry (0.5 H^+/electron) is lower than that of most other (mitochondrial-like) oxidases characterized to date (1 H^+/electron). We studied the pH dependence and deuterium isotope effect of the kinetics of electron and proton transfer reactions in the ba_3 oxidase. The results from these studies suggest that the movement of protons to the catalytic site and movement to a site located some distance from the catalytic site [proposed to be a "proton-loading site" (PLS) for pumped protons] are separated in time, which allows individual investigation of these reactions. A scenario in which the uptake and release of a pumped proton occurs upon every second transfer of an electron to the catalytic site would explain the decreased proton pumping stoichiometry compared to that of mitochondrial-like oxidases.

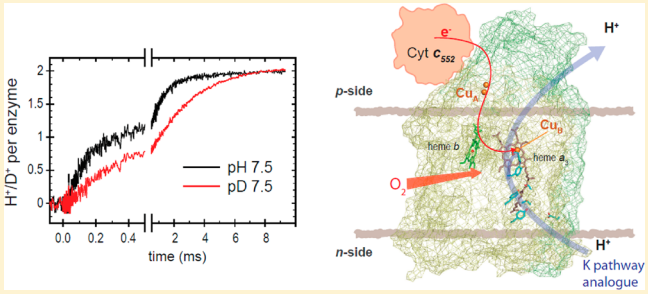

Cytochrome *c* oxidases (CytcOs) are membrane-bound enzymes that catalyze reduction of O_2 to H_2O. These enzymes are characterized by a catalytic site, which consists of a copper ion (Cu_B) and a heme group, where O_2 binds and is reduced by four electrons to water:

$$4e^- + 4H^+ + O_2 \rightarrow 2H_2O \quad (1)$$

This chemical reaction is arranged topographically such that electrons and protons are transferred from opposite sides of the membrane to the catalytic site, yielding a charge separation that is equivalent to that for moving a positive charge from the more negative (n) to the more positive (p) side of the membrane. In addition, most CytcOs studied to date are proton pumps, which couple the transfer of electrons to O_2 to translocation of protons across the membrane:

$$4e_p^- + 4(1 + n)H_n^+ + O_2 \rightarrow 2H_2O + 4nH_p^+ \quad (2)$$

where the subscripts refer to the two sides of the membrane and n is the number of protons translocated across the membrane (pumped protons) for each electron transferred to O_2. The free energy that is stored in the established electrochemical gradient is used, e.g., for transmembrane transport processes and ATP production. The electrons required for the reaction are delivered by cytochrome *c*, a small water-soluble protein residing on the p side, that docks to the CytcO and transfers one electron at a time to the Cu_A site. From there, electrons are transferred one by one, via a low-spin heme, to the catalytic site, consisting of a high-spin heme and Cu_B. Protons are taken up from the n side and transferred through the membrane-spanning part of the CytcOs, via specific proton pathways that are composed of polar and protonatable residues as well as water molecules (refs 1−6 describe this process in detail).

The bacterial CytcOs from, for example, *Rhodobacter sphaeroides* and *Paracoccus denitrificans*, as well as the mitochondrial CytcO, bind two A-type hemes, a low-spin heme *a* and a high-spin heme a_3, and are termed aa_3 CytcOs. The bacterial aa_3 CytcOs harbor two proton uptake pathways denoted by letters D (after a conserved Asp residue near the entrance of the pathway) and K (after a conserved Lys residue within the pathway).[7−13] Analogously, the D and K pathways are also found in the mitochondrial CytcO. However, in the mitochondrial enzyme, a third (H) pathway has been proposed to be used for transfer of pumped protons across the membrane.[14] The K pathway is required for the uptake of only two "substrate protons" upon reduction of the catalytic site[15−17] (see also ref 18) (a substrate proton is defined as a proton that is used for reduction of dioxygen to water at the

Received: January 30, 2012
Revised: May 10, 2012
Published: May 24, 2012

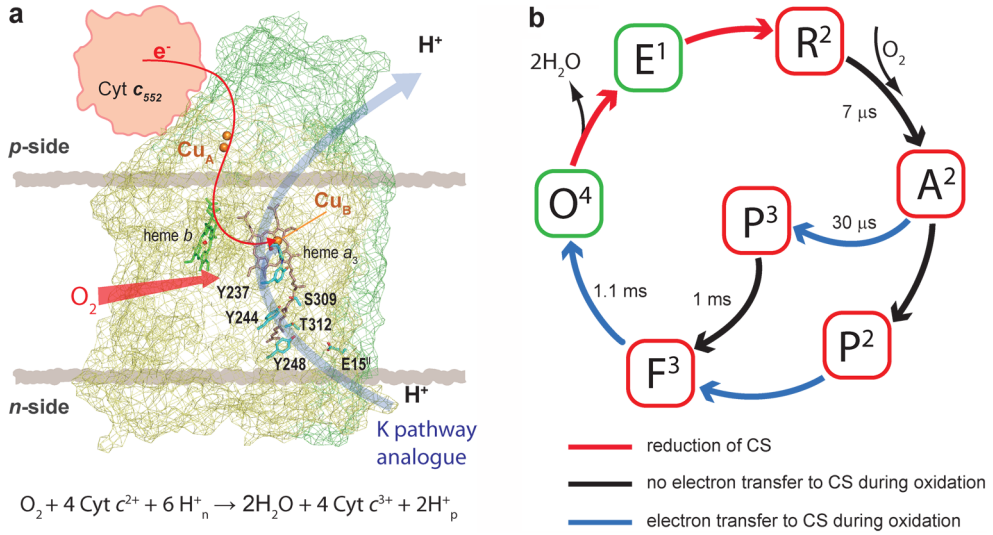

Figure 1. Structure and O_2 reduction mechanism of the ba_3 *T. thermophilus* CytcO. (a) Schematic representation and overall mechanism of the *T. thermophilus* ba_3 oxidase.[21] Electrons are transferred from a water-soluble cytochrome *c* to the primary electron acceptor Cu_A and then via heme *b* to the catalytic site (see the red arrow), composed of heme a_3 and Cu_B, where O_2 binds and is reduced to H_2O. Protons are taken up from the n side, via a single proton pathway, and are delivered to the catalytic side as well as to a proton-loading site (PLS) from which they are released to the p side. Proposed key residues of the proton pathway are indicated. The overall reaction catalyzed by the ba_3 oxidase is depicted below the picture (subscripts n and p refer to the two sides of the membrane). (b) Schematic reaction cycle of the ba_3 oxidase. The different states of the CytcO are indicated by the one-letter codes, where the superscript indicates the number of electrons transferred to the catalytic site. With the fully oxidized enzyme (state $\mathbf{O^4}$, equivalent to $\mathbf{O^0}$) as a starting point, consecutive reduction of the catalytic site (CS) by two electrons renders $\mathbf{R^2}$ (via $\mathbf{E^1}$), where O_2 binds. This binding is followed in time by splitting of the O−O bond and formation of the "peroxy" ($\mathbf{P^2}$) state. With the four-electron reduced CytcO ($\mathbf{R^2}$ plus one electron on Cu_A and one electron on heme *b*) as a starting point, an electron is transferred from heme *b* to the catalytic site forming state $\mathbf{P^3}$ that is chemically similar to $\mathbf{P^2}$ but carries one more electron. Both $\mathbf{P^3} \rightarrow \mathbf{F^3}$ and $\mathbf{P^2} \rightarrow \mathbf{F^3}$ reactions involve the transfer of a proton to the catalytic site, but only the $\mathbf{P^2} \rightarrow \mathbf{F^3}$ reaction involves the transfer of an electron to the catalytic site. The $\mathbf{F^3} \rightarrow \mathbf{O^4}$ reaction involves the transfer of an electron and a proton to the catalytic site as well as proton pumping. Proton uptake and pumping events are not indicated in that scheme. Color codes of the arrows are explained below the scheme. Green and red boxes depict states in the reductive and oxidative half-cycles of the reaction, respectively.

catalytic site of CytcO), while the six remaining protons (two substrate protons and all four pumped protons) are transferred through another, D (or H) pathway.[16,19,20] These aa_3 oxidases pump on average one proton per electron transferred to the catalytic site (i.e., $n = 1$ in eq 2).

The ba_3 CytcO from *Thermus thermophilus* is expressed at high temperatures and low oxygen concentrations and displays a low level of sequence identity to the mitochondrial-like CytcOs. However, the overall structural assembly as well as the distances between the redox centers is very similar to that of the mitochondrial-like enzymes. As the name indicates, the ba_3 CytcO contains a low-spin heme *b* replacing heme *a*. The crystal structures of the ba_3 CytcO from *T. thermophilus* revealed several putative proton pathways,[21−24] but only one of these has been suggested to be functional[23] (see also ref 25). This pathway is located at a position in space that is equivalent to that of the K pathway in the oxidases discussed above (Figure 1a). This K pathway analogue is thus used for the transfer of both substrate protons to the catalytic site and the uptake of protons to be pumped from the n side of the membrane. The reaction of fully reduced ba_3 CytcO with oxygen and internal electron transfer reactions have been investigated, suggesting a basic sequence similar to that of the aa_3-type oxidases.[26−31] In the reaction of the four-electron-reduced ba_3 CytcO with O_2, initially, oxygen binds to the reduced catalytic site (state $\mathbf{R^2}$, where the superscript indicates the number of electrons added to the oxidized catalytic site, in the reduced CytcO one electron each at heme a_3 and Cu_B) with formation of the intermediate $\mathbf{A^2}$ (O_2 bound to heme a_3) ($k \cong 1.7 \times 10^8$ M^{-1} s^{-1},[29] but see refs 32 and 33).[29] Next, three electrons are taken from the catalytic site and one is taken from heme *b*, associated with breaking of the O−O bond, forming a ferryl state, for historical reasons denoted "peroxy" (termed $\mathbf{P^3}$, or $\mathbf{P_R}$) with a time constant of ∼15 μs. In the next step, a proton is taken from the solution and the electron on Cu_A is transferred to heme *b* with a time constant of 30−70 μs. Finally, the fully oxidized state is formed concomitantly with the uptake of the second proton from the solution with a time constant of ∼1 ms (at pH 7.5). The major difference from the aa_3-type CytcOs is that in the ba_3 CytcO, no intermediate with a spectrum indicating a ferryl state denoted **F** (here $\mathbf{F^3}$) is formed at pH 7.5.[29] Because in the aa_3 CytcOs the absorbance changes characteristic of state $\mathbf{F^3}$ are attributed to transfer of a proton to the catalytic site, the proton taken up concomitantly with heme *b* re-reduction in the ba_3 CytcO presumably resides at a location distant from the catalytic site[31] (see also ref 29). Also, the proton pumping stoichiometry is lower, and on average, 0.5 proton is pumped per electron transferred to the catalytic site (i.e., $n = 0.5$ in eq 2).[34,35]

As mentioned above, in the bacterial aa_3 CytcOs all protons that are pumped are transferred through the D pathway. In these CytcOs, the branching point from where protons are transferred either to the catalytic site or to an acceptor site for the pumped protons [defined as the proton-loading site (PLS); see, for example, ref 36) is located at a highly conserved glutamate residue, Glu286 (*R. sphaeroides* numbering).[7] Because only a single pathway is used in the ba_3 CytcO, a branching point from where protons are transferred either to

dx.doi.org/10.1021/bi300132t | *Biochemistry* 2012, 51, 4507−4517

the catalytic site or to the PLS must exist in this pathway as well. The identity or location of this site is presently unknown; there is no acidic residue equivalent to Glu286 in the ba_3 oxidase.

Here, using microsecond resolution spectroscopy, we investigated electron and proton transfer reactions occurring upon the oxidation of the reduced ba_3 Cyt*c*O by O_2 as a function of pH, as well as the solvent isotope effect in this reaction.

MATERIALS AND METHODS

Purification of ba_3 Cyt*c*O. His-tagged wild-type Cyt*c*O was expressed and purified as described previously.[31] The purified protein was kept at 4 °C in 5 mM Hepes (pH 7.4) and 0.05% dodecyl β-D-maltoside (DDM) (Glycon).

Flash Photolysis Experiments. A sample containing ba_3 oxidase (6−7 μM enzyme) in 100 mM buffer (MES for pH 5.5−6, HEPES for pH 7−8, and CHES for pH 9−10), 0.05% DDM, and 0.1 mM EDTA was placed in an anaerobic cuvette, and the atmosphere was exchanged for N_2. Sodium dithionite was added (final concentration of ∼200 μM) before the atmosphere was exchanged for carbon monoxide. The reduction and CO binding processes were followed spectroscopically. Dissociation of the CO ligand was initiated by a short laser pulse (10 ns, 200 mJ, 532 nm, Nd:YAG laser from Quantel), and CO rebinding was followed at 445 nm with an oscilloscope (the experimental setup is described in ref 17).

Sample Preparation for Flow-Flash Measurements. A sample containing ba_3 oxidase [∼10 μM enzyme in 2 mM Hepes (pH 7.4) and 0.05% DDM] was placed in an anaerobic cuvette, and the atmosphere was exchanged for N_2 on a vacuum line. To reduce the enzyme, 0.5 μM PMS and 2 mM sodium ascorbate were added, and the sample was incubated until reduction of the enzyme was complete. The atmosphere was then exchanged for CO. Reduction and CO binding processes were followed spectroscopically.

For measurements in D_2O, the purified enzyme was concentrated in a centrifugal filter unit (Amicon Ultra, 0.5 mL, 100 kDa cutoff), and buffer was exchanged three times with 2 mM Hepes/K^+OD^- (KOH pellets dissolved in D_2O) (pD 7.5) and 0.05% DMM (dissolved in D_2O).

Flow-Flash Measurements. Measurements of the reaction of the reduced enzyme with oxygen were performed in a locally modified stopped-flow apparatus (Applied Photophysics) as described in ref 17. Briefly, the enzyme solution [2 mM Hepes (pH 7.5) and 0.05% DDM] was rapidly mixed in a 1:5 ratio with an oxygen-saturated solution [100 mM buffer (pH 5−11) and 0.05% DDM], and the reaction was initiated after 30 ms by flash photolysis (10 ns, 200 mJ, 532 nm, Nd:YAG laser, Quantel) of the enzyme−CO complex. The kinetic traces were recorded at given wavelengths on a digital oscilloscope.

The following buffers were used: citric acid (pH <5.5), MES (pH 5.5−6.5), HEPES (pH 7−8), CHES (pH 8.5−9.5), and CAPS (pH 10−11). For D_2O measurements, all the buffers were prepared in D_2O and the pH was adjusted with K^+OD^-.

Proton Uptake Measurements. The uptake of protons from the solution during oxidation was performed as described in ref 30. Briefly, the purified enzyme solution was run over a PD-10 column (GE Healthcare) and the buffer was exchanged for 150 mM KCl (pH ∼7.4) and 0.05% DDM. The protein was then diluted in the same solution to the appropriate concentration (∼10 μM) and placed in a Thunberg cuvette. In the stopped-flow apparatus, the enzyme was mixed in a 1:5 ratio with an unbuffered solution containing 150 mM KCl, 0.05% DDM, and 50 μM pH sensitive dye (phenol red for pH 6−8.5 and *m*-cresol purple for pH 8.5−10), and the absorption changes at 572 nm were followed. Quantification of proton uptake was performed via spectroscopic titration of the exhaust with defined additions of NaOH and HCl.[28]

For D^+ uptake measurements, the unbuffered enzyme was prepared as described above and the solvent was exchanged for 150 mM KCl and 0.05% DDM in D_2O in a centrifugal filter unit (Amicon Ultra, 0.5 mL, 100 kDa cutoff).

RESULTS

Binding of CO to Reduced ba_3 Cyt*c*O. To probe any protonation-linked changes at the catalytic site, we investigated the pH dependence of CO−ligand binding after flash photolysis of the complex between reduced ba_3 and CO using time-resolved optical absorption spectroscopy. The reactions were followed in time at 445 nm, where CO ligand binding results in absorbance changes. After flash photolysis of the CO ligand, triggered by a short laser pulse, an unresolved absorbance increase due to dissociation of the CO ligand from heme a_3 is observed (Figure 2a). This absorbance change was followed in time by a very small (∼5% of the total absorbance change) decrease in absorbance with a rate constant of ∼5500

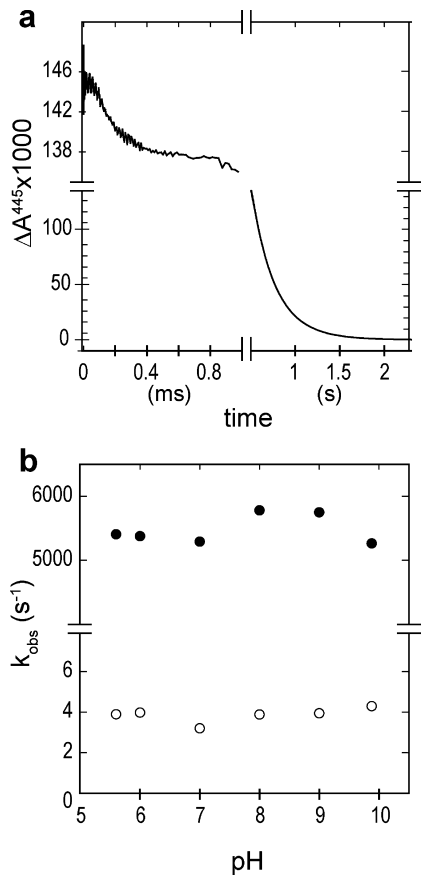

Figure 2. pH dependence of the CO recombination kinetics. (a) Absorbance changes at 445 nm associated with recombination of CO with heme a_3 in dithionite-reduced ba_3 oxidase at pH 7. CO rebinding is biphasic with rate constants of ∼5500 and ∼4 s^{-1}, accounting for ∼5 and ∼95% of the signal amplitude, respectively. (b) pH dependence of CO rebinding kinetics in the range between pH 5.6 and 10 [rapid phase (●) and slow phase (○)].

dx.doi.org/10.1021/bi300132t | *Biochemistry* 2012, 51, 4507−4517

Table 1. Summary of the Rate Constants of the Different Steps during the Reaction of the Four-Electron Reduced ba_3 CytcO with O_2[a]

reaction	wavelength (±increase/decrease)	rate (s^{-1}) (time constant) pH 7	pD 7	KIE[b]	pH 10
heme b → CS ($\mathbf{A^2} \rightarrow \mathbf{P^3}$ eT)	560 (−), 610 (+)	6.8×10^4 (15 μs)	6.5×10^4 (15 μs)		4.8×10^4 (21 μs)
Cu_A → heme b eT	560 (+), 830 (+)	$1.5–2.5 \times 10^4$ (40–67 μs)	$1.5–2.5 \times 10^4$ (40–67 μs)[c]		1.3×10^4 (80 μs)
first proton uptake	dye (+)	1.4×10^4 (71 μs)	4.5×10^3 (220 μs)	3.1	1.0×10^4 (100 μs)
decay of $\mathbf{P^3}$ (i.e., the $\mathbf{P^3} \rightarrow \mathbf{F^3}$ reaction)	610 (−)	1100 (0.91 ms)	450 (2.2 ms)	2.4	650 (1.5 ms)
formation of $\mathbf{F^3}$ (i.e., the $\mathbf{P^3} \rightarrow \mathbf{F^3}$ reaction)	580 (+)	1100 (0.91 ms)	nd	–	560 (1.8 ms)
second proton uptake (interpreted to be linked to the $\mathbf{P^3} \rightarrow \mathbf{F^3}$ reaction)	dye (+)	1100 (0.91 ms)	320 (3.1 ms)	3.3	450 (2.2 ms)
formation of $\mathbf{O^4}$ (heme b → CS eT)	560 (−)	850 (1.2 ms)	250 (4.0 ms)	3.4	100 (10 ms)

[a]Abbreviations: eT, electron transfer; CS, catalytic site; nd, not detected. Time constants [1/(rate constant)] are given in parentheses. [b]The KIE is not given for the first two (pure) electron transfer reactions. [c]A range is given for the Cu_A → heme b electron transfer as discussed in more detail in Discussion.

s^{-1} ($\tau \cong 180$ μs), presumably associated with dissociation of CO from Cu_B (after dissociation from heme a_3, the CO ligand binds transiently to Cu_B[37−39]), and a major decrease in absorbance with a rate constant of ∼4 s^{-1} ($\tau \cong 250$ ms), associated with recombination of the CO−heme a_3 complex. This rate constant is similar to that observed in one study[38] but slightly smaller than that observed in another study.[39] As seen in Figure 2b, both kinetic phases were independent of pH in the range from pH 5.5 to 10.

Reaction of Reduced ba_3 CytcO with O_2. We, as well as others, have previously investigated the reaction of the four-electron-reduced wild-type ba_3 CytcO with O_2 at neutral pH. On the basis of these studies, a reaction scheme similar to that observed with the aa_3 oxidases was formulated (see Figure 1b).[28−31,40]

We first discuss data obtained at pH 7 (Table 1). Figure 3a shows absorbance changes at 560 nm, where mainly heme b contributes. After CO dissociation at time zero, first O_2 binds with a time constant of ∼6 μs at 1 mM O_2[29] and then we observed a rapid decrease in absorbance ($\tau \cong 15$ μs) that is associated with oxidation of heme b and thus the transfer of an electron to the catalytic site. Results from earlier studies with the aa_3[41] and ba_3[28,29] CytcOs have shown that this electron transfer results in formation of the peroxy state, $\mathbf{P^3}$, at the catalytic site. This $\mathbf{P^3}$ state displays an absorption maximum near 610 nm,[25,29] and a fit of the kinetic difference spectrum associated with this phase,[29] obtained from the same type of experiment as described here, indicates that the same process is seen also at this wavelength. Accordingly, we did observe an increase in absorbance at 610 nm (Figure 3c) over the same time scale ($\tau \cong 15$ μs) as heme b oxidation, seen at 560 nm (Figure 3a).

Formation of the $\mathbf{P^3}$ state was followed in time by an increase in absorbance at 560 nm with a time constant of ∼70 μs (Figure 3a), which is associated with re-reduction of heme b. In addition, we observed an increase in absorbance at 830 nm with the same time constant (Figure 3d), which is associated with simultaneous oxidation of Cu_A. This reaction occurred over the same time scale as the uptake of protons from solution (measured at 572 nm with pH sensitive dyes, first component shown in Figure 4a). Siletsky et al. previously observed the same electron transfer reaction, although with a time constant of 29 μs, and a voltage change interpreted as proton uptake with a time constant of 46 μs.[29] Technically, we could also reproduce this difference in the time constants of the electron and proton transfer reactions; the former could be fit with a smaller time constant (∼40 μs) than the latter (∼70 μs). However, this difference in time constants between the electron and proton transfer reactions is not sufficient to argue that electron transfer is faster than proton transfer (but see data in D_2O below).

In the next step, the absorbance at 610 nm decreased with a time constant of ∼1 ms (Figure 3c), which coincided in time with an increase in absorbance at 580 nm (Figure 3b). The absorbance at 560 nm decreased with a similar time constant of ∼1 ms (oxidation of heme b). This reaction was also linked in time to the uptake of a proton from solution [second component (Figure 4a)]. The product that is formed is the oxidized CytcO ($\mathbf{O^4}$). In Figure S1 of the Supporting Information, absorbance changes at 430 nm, which mainly reports redox changes at heme b, and at 445 nm, which mainly reports changes at heme a_3, are shown. The rates determined from studies at these wavelengths coincide well with those found at 560 nm.

Below, we discuss each of the kinetic phases, along with their pH dependencies, in more detail. Representative traces obtained at pH 5, 7, 9, and 10 are shown in Figure 3, and the rates as a function of pH are plotted in Figure 5 (see also Table 1).

First Resolved Phase, the $\mathbf{A^2} \rightarrow \mathbf{P^3}$ Reaction. The first reaction phase observed in our experiments is the $\mathbf{A^2} \rightarrow \mathbf{P^3}$ reaction, which follows immediately after binding of O_2 to heme a_3 (i.e., formation of $\mathbf{A^2}$). The rate constant of the initial absorbance decrease at 560 nm (Figure 3a) and the absorbance increase at 610 nm (Figure 3c), associated with the transfer of an electron from heme b to the catalytic site and the $\mathbf{A^2} \rightarrow \mathbf{P^3}$ reaction, changed from ∼7×10^4 s^{-1} ($\tau \cong 13$ μs) at pH 4 to ∼4.8×10^4 s^{-1} ($\tau \cong 21$ μs) at pH 10; i.e., the rate displayed a very weak pH dependence (Figure 5a).

Transfer of an Electron from Cu_A to Heme b and the First Proton Uptake. The pH dependence of the transfer of an electron from Cu_A to heme b was obtained from the increase in absorbance at 560 nm [heme b re-reduction (Figure 3a)]. As seen in Figure 5b, this reaction rate displayed a very weak pH

dx.doi.org/10.1021/bi300132t | Biochemistry 2012, 51, 4507−4517

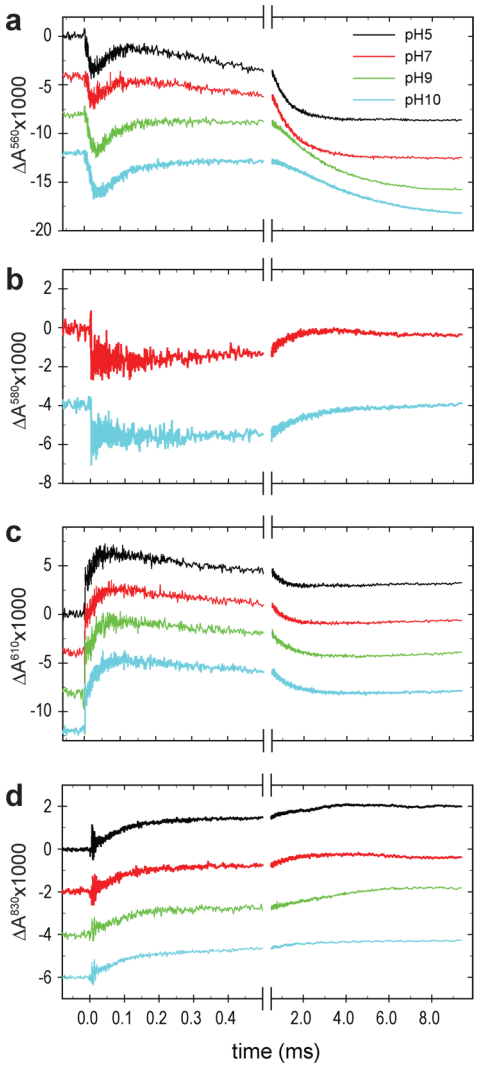

Figure 3. Absorbance changes associated with reaction of the fully reduced ba_3 CytcO with O_2 at different pH values: (a) 560 nm, representing redox reactions of heme *b*; (b) 580 nm, representing formation of state $\mathbf{F}^3$; (c) 610 nm, representing formation and decay of the $\mathbf{P}^3$ state (absorbance increase and decrease, respectively), and (d) 830 nm, representing the redox reaction of Cu_A. Experimental conditions after mixing: 100 mM buffer according to pH (see Materials and Methods), 0.05% dodecyl *β*-D-maltoside (DDM), and ~22 °C. The CO ligand was dissociated by a laser flash at time zero. Amplitudes are normalized to 1 *μ*M reacting ba_3 CytcO.

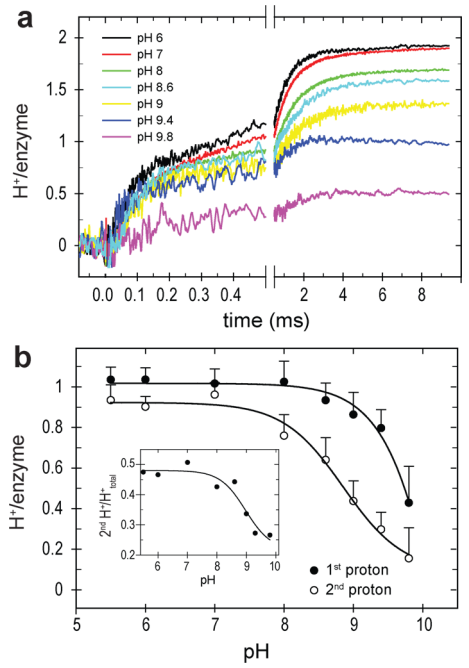

Figure 4. Uptake of protons from solution during the reaction of fully reduced ba_3 CytcO with O_2 at different pH values. (a) Absorbance changes of pH dyes phenol red and *m*-cresol purple at 572 nm during reaction of the reduced ba_3 CytcO with O_2 in the pH range of 6–9.8 (see also Materials and Methods). (b) Amplitudes of the two kinetic phases obtained from traces in panel a, first phase [average amplitude between 0 and 0.5–0.6 ms (●)] and second phase [average amplitude between 0.5–0.6 and 8–9 ms (○)]. Error bars represent averages from three different measurements from two preparations. The inset represents the ratio of the amplitude of the second phase to the total amplitude. Sigmoidal fits were calculated using SigmaPlot.

dependence in the pH range from 5 to 9 where the average rate was ~1.5×10^4 s^{-1} ($\tau \cong 67$ *μ*s). It decreased slightly above pH 10, reaching a value of ~9.8×10^3 s^{-1} ($\tau \cong 95$ *μ*s) at pH 11. As observed previously, this electron transfer was also linked in time to the uptake of a proton from solution[28,31] (Figure 4a). At all pH values (6.0–9.8), two kinetic proton uptake phases were observed. The rate of the first kinetic component displayed a very weak pH dependence up to pH 9, where the average rate was ~1.5×10^4 s^{-1} ($\tau \cong 67$ *μ*s) (Figure 5b). Above pH 9, the rates dropped slightly to 1×10^4 s^{-1} at pH 9.8 ($\tau \cong$ 100 *μ*s).

Second Proton Uptake. As discussed above, at neutral pH the reactions after re-reduction of heme *b* displayed very similar time constants of 1.0 ± 0.3 ms at all studied wavelengths (see Table 1 and Figure 3), thus consistent with a decay directly from $\mathbf{P}^3$ to $\mathbf{O}^4$. However, as reported previously,[31] at high pH values, faster rates were observed at 610 nm [interpreted as decay of state $\mathbf{P}^3$ (see Discussion)] than at 560 nm (final oxidation of the enzyme, i.e., formation of $\mathbf{O}^4$). In addition, the faster but not the slower of these processes coincided in time with the uptake of a proton from solution. The conclusion from our earlier studies was that at pH 7 the 1 ± 0.3 ms reaction reflects two distinct processes, which at higher pH values are separated in time.[31] These two processes are discussed in this and the next subsections.

The pH dependence of the rate constant of the absorbance decrease at 610 nm, together with the rate of proton uptake, is shown in Figure 5c. The two processes coincided well in time, and the rate exhibited a modest pH dependence; it decreased from ~1500 s^{-1} ($\tau \cong 0.7$ ms) at pH 5.5 to ~500 s^{-1} ($\tau \cong 2$ ms) at pH 11.

The $\mathbf{F}^3$ state displays a peak at 580 nm, relative to the oxidized state.[41,42] As seen in Figure 3b, we did observe an increase in absorbance at 580 nm and the rate constants were ~1100 s^{-1} ($\tau \cong 0.9$ ms) at pH 7 and 560 s^{-1} ($\tau \cong 1.8$ ms) at pH 10. These values are approximately the same as those observed at 610 nm and for the second phase of proton uptake (Figure 5c). Furthermore, at pH 10, the absorbance increase at 580 nm was faster than the absorbance decrease at 560 nm (10 ms). In other words, these data indicate that the increase in absorbance at 580 nm correlates in time with the decay of the $\mathbf{P}^3$ state (decrease in absorbance at 610 nm), but not formation of the oxidized state $\mathbf{O}^4$ (decrease in absorbance at 560 nm).

dx.doi.org/10.1021/bi300132t | *Biochemistry* 2012, 51, 4507–4517

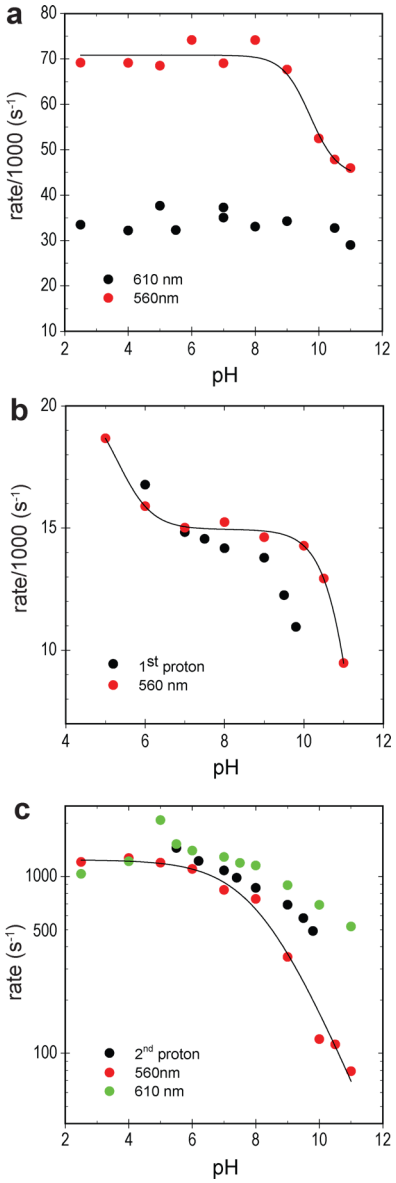

Figure 5. pH dependence of the rates of the different kinetic phases seen during reaction of reduced ba_3 CytcO with O_2 (see Figures 3 and 4). Shown are representative values for absorbance changes at 560 and 610 nm and proton uptake observed at 572 nm. Error bars were omitted for the sake of clarity, but rates vary by up to 20% between experiments from different protein preparations. (a) Initial oxidation of heme *b* at 560 nm (red circles, fitted to one sigmoidal line with a pK_a of 9.75). (b) Re-reduction of heme *b* at 560 nm (red circles, fitted to two sigmoidal lines with pK_a values of 5.3 and 11.5) and first phase of uptake of protons from solution (black circles). (c) Decay of $\mathbf{P}^3$ at 610 nm (red circles), second phase of uptake of protons from solution (black circles), and oxidation of heme *b* at 560 nm (blue circles, fitted to one sigmoidal line with a pK_a of 8.2).

Formation of Oxidized CytcO. The pH dependence of the final oxidation rate of the ba_3 oxidase, as determined from the slowest absorbance decrease at 560 nm [also seen at 430 and 445 nm (Figure S1 of the Supporting Information)], is shown in Figure 5c. As seen in this figure, the rate displayed a relatively strong pH dependence where the maximal and minimal rates were ~1300 s^{-1} ($\tau \cong 0.8$ ms) and ~80 s^{-1} ($\tau \cong 20$ ms) at pH 5.5 and 11, respectively. The pH dependence was fit with a Henderson–Hasselbalch titration curve with a pK_a of 8.2 (Figure 5c).

Proton Uptake. As mentioned above, two proton uptake reactions were observed; one coincided in time with the Cu_A-to-heme *b* electron transfer ($\tau \cong 70$ μs at pH 7) and the second with the decrease in absorbance at 610 nm [interpreted as the $\mathbf{P}^3 \rightarrow \mathbf{F}^3$ reaction (see Discussion)] ($\tau \cong 0.95$ ms at pH 7). As seen in Figure 4a at all pH values ranging from 6.0 to 9.8, two kinetic phases were observed. The rates of these components displayed very weak pH dependencies as outlined above (see Figure 5b,c). However, we did observe a significant decrease in the net proton uptake stoichiometry with increasing pH. As seen in Figure 4b, the first phase corresponded to a proton uptake stoichiometry of ~1 H^+/CytcO in the pH range of 5.5–9, after which the value decreased to 0.4 H^+/CytcO at pH 9.8. In contrast, the contribution of the second component decreased with an increasing pH already at lower pH, from ~0.9 H^+/CytcO at pH 6.0 to ~0.1 H^+/CytcO at pH 9.8. As seen in the inset of Figure 4b, the fraction of the slow component decreased from ~50% of the total amplitude at the lower pH values to ~25% at the highest value.

Solvent Kinetic Isotope Effect. We also investigated the effect of exchanging the H_2O solvent for D_2O on the CytcO reaction kinetics [kinetic isotope effect (KIE)] at pH/pD 7.5 (Figure 6a–d and Table 1). The $\mathbf{A}^2 \rightarrow \mathbf{P}^3$ reaction, as seen at 560 nm (initial absorbance decrease) and 610 nm (absorbance increase), displayed a KIE close to 1. In earlier studies with the *R. sphaeroides* aa_3 oxidase, a small KIE of ~1.8 at a pH meter reading of 7.5 was observed for this reaction and attributed to internal proton transfer within the catalytic site upon formation of $\mathbf{P}^3$.[43]

The transfer of an electron from Cu_A to heme *b* (increase in absorbance at 830 and 560 nm) in H_2O linked in time to the first proton uptake with a rate constant of ~1.5×10^4 s^{-1} ($\tau \cong 70$ μs) was biphasic in D_2O. In D_2O, the first phase (90% of the amplitude) displayed a rate constant of ~2.5×10^4 s^{-1} ($\tau \cong 40$ μs) while the second phase was slower and linked in time to the uptake of a proton from solution with a rate constant of 4500 s^{-1} ($\tau \cong 220$ μs); i.e., it displayed a KIE of ~3. Thus, the slower, but not the faster, of these components displayed a rate constant that was the same as that of proton uptake in D_2O.

The absorbance decrease at 610 nm displayed a KIE of 2.4 at both pH 6 and 10.5. The associated second proton uptake displayed a KIE of ~3.3. The final oxidation of the CytcO displayed a KIE of ~3.3 at both pH 6 and 10.5.

DISCUSSION

The results from this study as well as previous studies of the *T. thermophilus* ba_3 CytcO[26−31] indicate that the overall sequence of reactions during oxidation of this enzyme is similar to that found with the aa_3 CytcOs. However, the timing is different as is the sequence of the proton uptake reactions and proton pumping events. Heme *b* oxidation [as seen at 560 nm (Figure 3a)] and formation of the $\mathbf{P}^3$ state [as seen at 610 nm (Figure 3c)] occur with a time constant of ~15 μs, which is faster than with, e.g., the *R. sphaeroides* aa_3 CytcO. This observation is noteworthy given the fact that the ba_3 CytcO normally operates at temperatures much higher than those used in the experiments presented here (at higher temperatures, the formation rate of $\mathbf{P}^3$ would presumably be even faster).

In the steps following in time after $\mathbf{P}^3$ formation, the situation is distinctly different in the aa_3 and ba_3 oxidases. In the *R. sphaeroides* aa_3 CytcO, after formation of $\mathbf{P}^3$ a proton is

dx.doi.org/10.1021/bi300132t | *Biochemistry* 2012, 51, 4507–4517

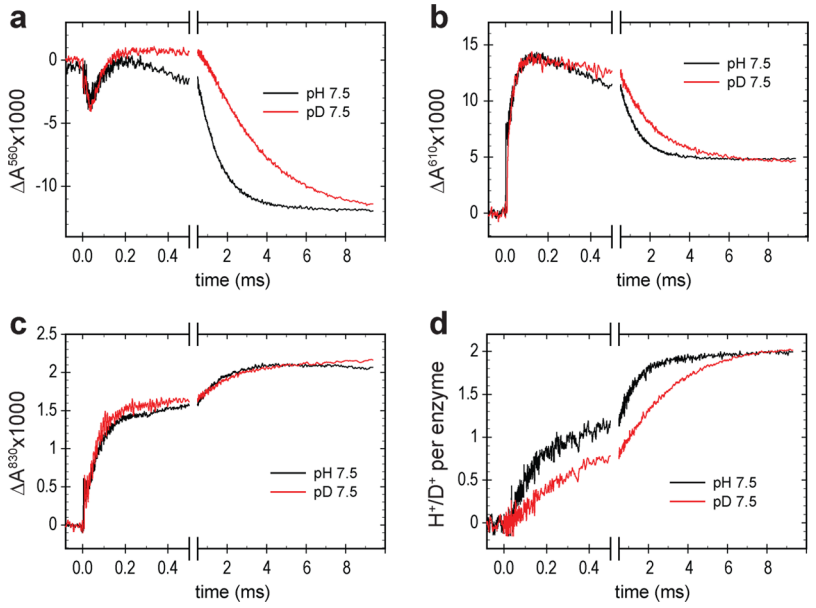

Figure 6. Kinetic isotope effects for the reaction of the fully reduced ba_3 with O_2. Shown are the comparisons of the reaction in H_2O at pH 7.5 (black line) and D_2O at pD 7.5 (red line). See Materials and Methods for experimental details: (a) 560 nm, representing redox reactions of heme *b*; (b) 610 nm, representing formation and decay of $\mathbf{P}^3$; (c) 830 nm, representing the redox reaction at Cu_A, and (d) uptake of a proton from solution measured with the pH sensitive dye phenol red. Absorbance changes were converted to H^+/D^+ per enzyme as described in Materials and Methods.

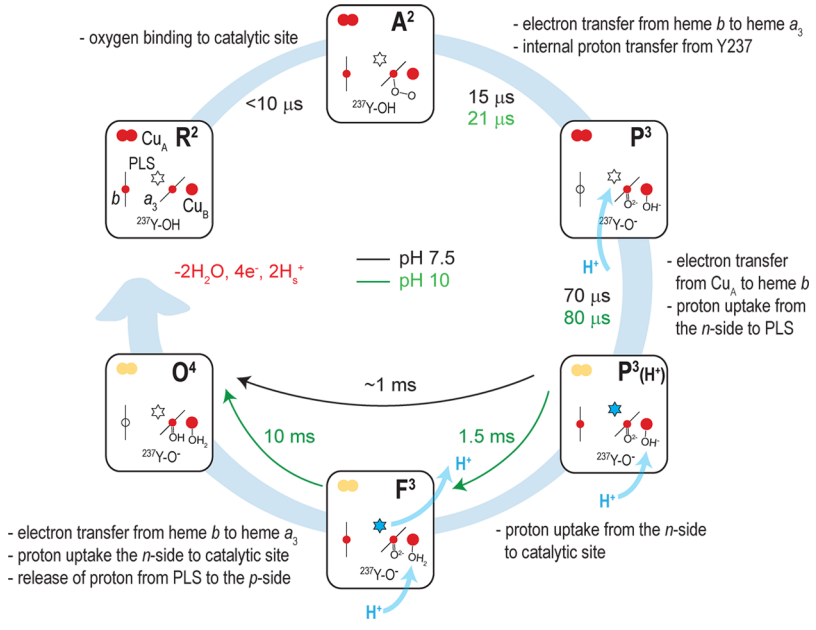

Figure 7. Working model for the reaction of the fully reduced ba_3 CytcO with O_2. With $\mathbf{R}^2$ (with additional electrons on Cu_A and heme *b*) as a starting point, oxygen binds to the reduced catalytic site. Upon transfer of an electron form heme *b* to the catalytic site and an internal transfer of a proton from the catalytically important Tyr237 (^{237}Y-OH), the oxygen bond is broken and state $\mathbf{P}^3$ is formed. Up to this point, the mechanism is similar to that of the aa_3 oxidases. Next, according to our data, the transfer of an electron from Cu_A to heme *b* is accompanied by the uptake of a proton by a site distant from the catalytic site, presumably the loading site for a pumped proton (PLS, indicated by a star), indicated as state $\mathbf{P}^3(\mathbf{H}^+)$. In the next step, a second proton is taken up by the catalytic site forming $\mathbf{F}^3$. In the final step, the transfer of an electron from heme *b* to the catalytic site and proton uptake as well as proton pumping take place (as observed via electrometric measurements[29]). At neutral pH values, the $\mathbf{P}^3(\mathbf{H}^+) \rightarrow \mathbf{F}^3$ and $\mathbf{F}^3 \rightarrow \mathbf{O}^4$ reactions have similar rates constants and cannot be kinetically resolved. Release of the two water molecules is triggered upon reduction of the fully oxidized state $\mathbf{O}^4$ ($\mathbf{O}^0$). To form $\mathbf{R}^2$, two electrons are transferred to the catalytic site and two additional electrons are transferred to heme *b* and Cu_A, respectively. Two substrate protons are taken up, and presumably, one pumped proton is taken up and released at the other side of the membrane.

taken up by the catalytic site to form $\mathbf{F}^3$, as well as the uptake and release of a proton that is pumped across the membrane (all with a time constant of ~100 μs at pH 7[44,45]). In the ba_3 Cyt*c*O, formation of $\mathbf{P}^3$ with a time constant of ~15 μs is also followed in time by proton uptake, here with a time constant of ~70 μs. However, this 70 μs reaction does not lead to absorbance changes at 580 nm that would be characteristic of formation of state $\mathbf{F}^3$, as convincingly shown by recording

dx.doi.org/10.1021/bi300132t | *Biochemistry* 2012, 51, 4507−4517

kinetic difference spectra during the reaction of the reduced ba_3 Cyt*c*O with O_2.[29] As also pointed out by Siletsky et al. in the aa_3 Cyt*c*Os, the proton that is taken up during the $\mathbf{P^3} \rightarrow \mathbf{F^3}$ reaction is presumably transferred to a hydroxide ion bound to Cu_B, which is proposed to lead to the absorbance increase at 580 nm. However, there is also a second available protonation site at the catalytic site, a Tyr residue (Y237), which is covalently bound to His333, one of the Cu_B ligands.[21] Siletsky et al. suggested that in the ba_3 Cyt*c*O, the proton would be transferred to the Tyr rather than to the hydroxide ion at Cu_B over a time scale of ~46 μs (time scale of ~70 μs observed in this work). They reasoned that because the Tyr site is located some distance from heme a_3, protonation of this site would not lead to absorbance changes characteristic of formation of the $\mathbf{F^3}$ state. In a more recent study, we suggested that the proton is rather transferred to a site outside of the catalytic site.[31] In other words, we offered a similar explanation for the absence of $\mathbf{F^3}$-specific absorbance changes at 580 nm; Siletsky et al.[29] suggested the transfer of a proton to Y237, while we proposed that the 70 μs proton is transferred to a site outside of the catalytic site. Our alternative conclusion is based on results from studies of the reaction of the three-electron-reduced ba_3 Cyt*c*O with O_2. From studies with the aa_3 oxidase, it is known that this reaction stops at the $\mathbf{F^3}$ state and cannot proceed to the $\mathbf{O^4}$ state because of the lack of a fourth electron. After transfer of all three electrons to the catalytic site to form state $\mathbf{P^3}$ in the ba_3 oxidase, two distinct proton uptake phases were observed with time constants of ~70 μs and ~1 ms.[31] Only the second proton uptake phase coincided in time with the decay in absorbance at 610 nm and an absorbance increase at 580 nm, suggesting that the second, but not the first, proton is transferred to the catalytic site to form $\mathbf{F^3}$. Because a total of one proton is expected to be transferred to the catalytic site after the transfer of an electron from heme *b*, we proposed that the first proton (~70 μs) is transferred to a site some distance from the catalytic site. In other words, the state of the catalytic site after the 70 μs proton uptake would still be $\mathbf{P^3}$, but we call it $\mathbf{P^3}(\mathbf{H^+})$ to emphasize that one additional proton is present within the Cyt*c*O. Because any proton pump must harbor a protonatable site having alternating access to the two sides of the membrane,[46] we speculated that the site mentioned above outside of the catalytic site is the loading site for pumped protons, previously denoted PLS (Figure 7) when discussed for the aa_3 oxidases (see the introductory section).

In this study, at pH 7 we observed an increase in absorbance at 580 nm (Figure 3b) and a decrease in absorbance at 610 nm (Figure 3c) with a time constant of ~1 ms, which was concomitant with the second proton uptake (Figures 4 and 5) (see also the summary in Table 1). Even though at pH 7 all these absorbance changes coincide in time with the final oxidation of the ba_3 Cyt*c*O, at high pH, oxidation of the Cyt*c*O occurs after these events (see Table 1). Hence, taken together with the data obtained with the three-electron-reduced Cyt*c*O as discussed above, we conclude that after the formation of $\mathbf{P^3}$, the first proton ($\tau \cong 70$ μs) is transferred to a site some distance from the catalytic site [state $\mathbf{P^3}(\mathbf{H^+})$] and $\mathbf{F^3}$ is formed with a time constant of ~1 ms (at pH 7 and 10). The final oxidation of the Cyt*c*O (formation of $\mathbf{O^4}$) occurs over the same time scale as formation of $\mathbf{F^3}$ at pH 7, which is the reason why the state is not populated to any significant extent. At pH 10, the final oxidation of the ba_3 Cyt*c*O is slower ($\tau \cong 10$ ms) than formation of $\mathbf{F^3}$.

We note that the absorbance at 580 nm does not decrease on the time scale over which we propose decay of the $\mathbf{F^3}$ state, as is observed with the aa_3 oxidases. The reason may be that this reaction is linked to oxidation of heme *b* rather than heme *a* and these two hemes display significantly different redox spectra at 580 nm.

We also note that the CO recombination data (see Figure 2) indicate that there are no protonation-dependent structural changes at the catalytic site of the *T. thermophilus* ba_3 Cyt*c*O that would affect ligand dissociation or binding, which is also in agreement with the finding that binding of CO to Cu_B is independent of pD.[39] These results suggest that the effects of pH changes on specific steps during reaction of the reduced Cyt*c*O with O_2 are not influenced by any protonation-dependent changes at the catalytic site itself.

Formation of the $\mathbf{P^3}$ state displayed a very weak pH dependence where the rate decreased by a factor of <2 with an increase in pH from 6 to 11 (Figure 5a). This very weak pH dependence is consistent with that observed for, e.g., the mitochondrial and *R. sphaeroides* aa_3 Cyt*c*Os, and the absence of any proton uptake or release during this reaction.[47,48] The $\mathbf{A^2} \rightarrow \mathbf{P^3}$ step does involve an internal transfer of a proton from Tyr288 (Tyr237 in ba_3) to the O_2 molecule at heme a_3 in the aa_3 Cyt*c*O. The rate of this proton transfer in the aa_3 Cyt*c*O was found to display a small KIE of 1.8.[43] In the ba_3 Cyt*c*O, the KIE of the $\mathbf{A^2} \rightarrow \mathbf{P^3}$ reaction was close to unity. This finding is qualitatively consistent with the faster formation of $\mathbf{P^3}$ in the ba_3 than in the aa_3 Cyt*c*O because the KIE typically decreases with an increase in the driving force of a proton transfer reaction.

With the ba_3 Cyt*c*O, the rate of the first proton uptake ($\tau \cong 70$ μs at pH 7) and the associated transfer of an electron from Cu_A to heme *b* displayed only a very weak pH dependence (Figure 5b). In contrast, with the aa_3 Cyt*c*Os discussed above, the first kinetic phase that involves proton uptake is pH-dependent above pH ~9 and displays a Henderson–Hasselbalch titration with a pK_a of 9.4. This pK_a is attributed to the protonation state of the Glu286 residue.[49] According to this model, the proton transfer rate is determined by the protonation fraction of the Glu residue.[49] The very weak pH dependence for the rate of proton uptake in the ba_3 Cyt*c*O can be explained using the same model, but assuming that the protonatable group within the K proton pathway analogue displays a pK_a that is outside of (above) the measured pH range. In fact, some single-site mutations in the D pathway of the *R. sphaeroides* and *P. denitrificans* Cyt*c*Os result in an elevation of the Glu286 pK_a such that the proton uptake rate becomes pH-independent in the experimentally available pH range.[50,51] Thus, the behavior of these mutant Cyt*c*Os is qualitatively the same as that of the ba_3 Cyt*c*O, i.e., a proton uptake reaction displaying pH-independent kinetics. The structural reason for the difference between the aa_3 and ba_3 Cyt*c*Os may be that in the latter case there is no protonatable group in the K pathway analogue that would act as a transient proton donor or acceptor on the pathway to the catalytic site in the pH range in which our measurements were taken. The K pathway analogue starts at Glu15 near the n side surface, but above this site, there are no other acidic or basic amino acid residues; the only protonatable residues are tyrosines. Even if one Tyr residue near the catalytic site has been found to have a pK_a in the pH range of our measurements,[25] it is likely that in the protein environment typically these groups have pK_a values of >10. Alternatively, proton uptake may be rate-limited by

another reaction, such as, for example, a structural change, that displays pH-independent kinetics. We also note that the 70 μs proton uptake did display a larger (~3) deuterium KIE than the preceding phase (~1). However, such a small KIE cannot be used to distinguish between the rate-limiting structural change of a protonatable site and rate-limiting proton transfer.

The data show that after the initial oxidation of heme *b*, in D_2O, the electron at Cu_A equilibrated with heme *b* with time constants of ~40 μs (90% of the total amplitude) and 220 μs. The first phase is faster than proton uptake in D_2O ($\tau \cong 220$ μs), which suggests that the electron equilibrates between Cu_A and heme *b* in a manner independent of proton uptake, but proton binding shifts this equilibrium further toward heme *b* over a time scale of ~220 μs. In H_2O, this proton uptake is faster than in D_2O, and therefore, it coincides in time with the transfer of an electron from Cu_A to heme *b*. In this context, it should be mentioned that also in H_2O it is possible to fit the electron transfer with a time constant of ~40 μs (see Results), which would yield a KIE of ≅1 for the transfer of an electron from Cu_A to heme *b* (the KIE for the proton transfer is ~3).

The rate of the absorbance decay at 610 nm (Figure 3c) or the second proton uptake (Figure 4), associated with the decay of the $\mathbf{P}^3(\mathbf{H}^+)$ state and formation of $\mathbf{F}^3$ with a time constant of ~1 ms at pH 7, displayed a relatively modest pH dependence, where the rate decreased by a factor of ~3 over the pH range from 5.5 to 11 (Figure 5c). This reaction also displayed a significant KIE of ~3. The difference in the pH dependencies for the two proton uptake kinetic phases is presumably due to differences in the details of the proton transfer trajectories for these reactions (transfer of a proton to PLS or the catalytic site) as well as differences in the driving force (i.e., the difference in pK_a between the proton donor and acceptor). As discussed above, we propose that, while the first proton is transferred to the PLS, the second one is transferred to the catalytic site (see Figure 7).

Given the very modest pH dependencies for the first two components, linked to the uptake of a proton from solution, it is surprising to note that the rate of the last component ($\mathbf{F}^3 \rightarrow \mathbf{O}^4$ reaction) displayed a significant pH dependence even though the reaction was not linked in time to any net uptake of protons from solution. Despite this absence of proton uptake, it is clear that the $\mathbf{F}^3 \rightarrow \mathbf{O}^4$ reaction requires the transfer of a proton to the catalytic site (see refs 3 and 52). The absence of any net proton uptake from solution was previously explained in terms of simultaneous release of a pumped proton from the PLS during the $\mathbf{F}^3 \rightarrow \mathbf{O}^4$ transition (cf. the proton that was taken up by the PLS during the 70 μs reaction).[31] This interpretation is consistent with results from earlier electrometric studies in which changes in voltage linked to internal electron and proton transfer reactions were studied.[29] These results showed that over a time scale of 50 μs (same phase as 70 μs in this work), one proton is transferred a distance of ~70% across the membrane, which was interpreted in terms of the transfer of a proton to the catalytic site, but the observation is also fully consistent with the transfer of a proton to a PLS, if this site is located slightly above the catalytic site. Furthermore, in the last phase of the reaction, attributed to formation of the $\mathbf{O}^4$ state, voltage changes corresponding to transfer of one charge across the membrane and one charge to the catalytic site were observed. According to our interpretation (see Figure 7), around neutral pH, over this time scale two protons would be transferred to the catalytic site, while one proton would be released from the PLS, which is expected to generate the same net voltage changes.

An important difference between the $\mathbf{F}^3 \rightarrow \mathbf{O}^4$ reaction and the preceding steps that involve proton uptake is that only in the $\mathbf{F}^3 \rightarrow \mathbf{O}^4$ reaction is the presumed proton uptake linked to the simultaneous transfer of an electron to the catalytic site. Results from experiments with the *R. sphaeroides* and *P. denitrificans* aa_3 CytcOs indicate that the rate of this electron transfer and the accompanying proton transfer to the catalytic site may be controlled by the release of the "pumped proton" from the PLS[53] (see also ref 54). Because in the ba_3 CytcO, during reaction of the reduced CytcO and O_2, only the $\mathbf{F}^3 \rightarrow \mathbf{O}^4$ reaction is linked to such a proton release,[29] the stronger pH dependence of the $\mathbf{F}^3 \rightarrow \mathbf{O}^4$ kinetics could reflect the pH dependence of the transfer of a proton from the PLS to the p side of the membrane.

As seen in Figure 4, the net proton uptake stoichiometry during the reaction of the reduced CytcO and O_2 decreased with an increase in pH. This decrease is mainly attributed to a decrease in the second proton uptake phase (see the inset of Figure 4b), while the amplitude of the first proton uptake phase was relatively unaltered below pH 9.4. Results from early studies with the mitochondrial bovine heart CytcO showed that the proton uptake stoichiometry decreased with an increase in pH for the $\mathbf{P}^3 \rightarrow \mathbf{F}^3$ and $\mathbf{F}^3 \rightarrow \mathbf{O}^4$ kinetic phases.[47,55] A lower proton uptake stoichiometry during oxidation of the CytcO must imply that the proton uptake stoichiometry upon reduction is larger (a net total of four protons must be taken up to reduce O_2 to H_2O, i.e., during reduction and oxidation of the CytcO).[47]

As discussed above, with the ba_3 CytcO, the first proton uptake component ($\tau \cong 70$ μs) presumably reflects the uptake of a proton by the PLS, while the second one reflects the transfer of a proton to the catalytic site. The relatively more significant decrease in the amplitude of the second proton uptake component with the ba_3 CytcO (see the inset of Figure 4b) is consistent with the observations made with the mitochondrial CytcO.[47] The unaltered stoichiometry for the first component may be explained in terms of a sufficiently large pK_a shift for the PLS such that in the pH range of 6−9.4 the protonation state of the PLS changes from unprotonated to 80−100% protonated after the transfer of an electron to the catalytic site (at the highest pH of 9.8, there is a decrease in the amplitude of the first component).

As discussed above, with, for example, the *R. sphaeroides* or *P. denitrificans* CytcOs, during turnover, in every reaction step that involves the transfer of an electron to the catalytic site, (i) a proton is taken up from the n side to the PLS, (ii) a proton is transferred to the catalytic site, and (iii) the proton at PLS is released to the p side. Also in the reaction of the four-electron-reduced aa_3 CytcO with O_2, after the transfer of an electron from heme *a* to the catalytic site (to form $\mathbf{P}^3$, as outlined above), proton transfer reactions i−iii (that occur during the $\mathbf{P}^3 \rightarrow \mathbf{F}^3$ reaction) all display the same time constant.[44,45] Thus, the order of proton transfer reactions is probably the most striking difference between the ba_3 CytcO and, for example, the *R. sphaeroides* and *P. denitrificans* aa_3 CytcOs.

The marked separation in time of the transfer of a proton to and from the PLS might be related to the presence of only one proton pathway in the ba_3 CytcO, because in all CytcOs the proton is both the ion that is translocated (pumped) and the ion that is used as a substrate for the reaction that drives pumping (i.e., O_2 reduction). Consequently, when using only

one proton pathway, it is important to ensure that the proton that is pumped across the membrane is separated in space and time from the substrate proton; otherwise, the free energy available for pumping would be lost. Furthermore, as for any ion pump, the flow of pumped protons across the membrane must be gated to ensure unidirectionality. A clear separation in time of the proton loading event to the PLS ($\tau \cong 70\ \mu s$) and the transfer of a proton to the catalytic site ($\tau \cong 1$ ms) may facilitate proton gating as outlined above. The price paid for this adjustment of the pumping mechanism is a lower pumping stoichiometry because a pumped proton is taken up or released for every second electron transfer to the catalytic site (see a more detailed discussion in ref 40). At the same time, this mechanism allows studies of the transfer of protons to the catalytic site and the PLS separately, which in future studies is expected to offer further insights into the functional design of the pump.

■ ASSOCIATED CONTENT

Supporting Information

Kinetic traces at 430 and 445 nm. This material is available free of charge via the Internet at http://pubs.acs.org.

■ AUTHOR INFORMATION

Corresponding Author

*Phone: +46 8 163280. Fax: +46 8 153679. E-mail: peterb@dbb.su.se.

Funding

These studies were supported by grants from the Swedish Research Council. C.v.B. was supported by a fellowship from the Swiss National Science Foundation (SNF).

Notes

The authors declare no competing financial interest.

■ ABBREVIATIONS

Cyt*c*O, cytochrome *c* oxidase; n and p sides, negative and positive sides of the membrane, respectively. Intermediate states that appear during turnover of the Cyt*c*O (the superscript indicates the number of electrons added to the oxidized catalytic site): $\mathbf{R^2}$, reduced catalytic site (one electron each added to heme a_3 and Cu_B); $\mathbf{A^2}$, O_2 bound to heme a_3 at the reduced catalytic site; $\mathbf{P^2}$ (also $\mathbf{P_M}$), peroxy state formed upon reaction of the two-electron-reduced catalytic site with O_2; $\mathbf{P^3}$ (also $\mathbf{P_R}$), peroxy state formed upon reaction of O_2 with the reduced catalytic site, where an electron is transferred from heme *a* to the catalytic site at the same time that O_2 reduction occurs; $\mathbf{F^3}$, "ferryl" state at the catalytic site; $\mathbf{O^4}$, oxidized catalytic site (equivalent to $\mathbf{O^0}$). Time constants are given as $(\text{rate constants})^{-1}$.

■ REFERENCES

(1) Hosler, J. P., Ferguson-Miller, S., and Mills, D. A. (2006) Energy transduction: Proton transfer through the respiratory complexes. *Annu. Rev. Biochem. 75*, 165−187.

(2) Belevich, I., and Verkhovsky, M. I. (2008) Molecular mechanism of proton translocation by cytochrome c oxidase. *Antioxid. Redox Signaling 10*, 1−29.

(3) Ferguson-Miller, S., and Babcock, G. T. (1996) Heme/copper terminal oxidases. *Chem. Rev. 96*, 2889−2907.

(4) Wikström, M., and Verkhovsky, M. I. (2007) Mechanism and energetics of proton translocation by the respiratory heme-copper oxidases. *Biochim. Biophys. Acta 1767*, 1200−1214.

(5) Brzezinski, P., and Gennis, R. B. (2008) Cytochrome c oxidase: Exciting progress and remaining mysteries. *J. Bioenerg. Biomembr. 40*, 521−531.

(6) Kaila, V. R. I., Verkhovsky, M. I., and Wikström, M. (2010) Proton-coupled electron transfer in cytochrome oxidase. *Chem. Rev. 110*, 7062−7081.

(7) Iwata, S., Ostermeier, C., Ludwig, B., and Michel, H. (1995) Structure at 2.8 Å resolution of cytochrome c oxidase from *Paracoccus denitrificans*. *Nature 376*, 660−669.

(8) Svensson-Ek, M., Abramson, J., Larsson, G., Törnroth, S., Brzezinski, P., and Iwata, S. (2002) The X-ray Crystal Structures of Wild-Type and EQ(I-286) Mutant Cytochrome *c* Oxidases from *Rhodobacter sphaeroides*. *J. Mol. Biol. 321*, 329−339.

(9) Tsukihara, T., Aoyama, H., Yamashita, E., Tomizaki, T., Yamaguchi, H., Shinzawa-Itoh, K., Nakashima, R., Yaono, R., and Yoshikawa, S. (1996) The whole structure of the 13-subunit oxidized cytochrome c oxidase at 2.8 Å. *Science 272*, 1136−1144.

(10) Liu, J., Qin, L., and Ferguson-Miller, S. (2011) Crystallographic and online spectral evidence for role of conformational change and conserved water in cytochrome oxidase proton pump. *Proc. Natl. Acad. Sci. U.S.A. 108*, 1284−1289.

(11) Qin, L., Hiser, C., Mulichak, A., Garavito, R. M., and Ferguson-Miller, S. (2006) Identification of conserved lipid/detergent-binding sites in a high-resolution structure of the membrane protein cytochrome c oxidase. *Proc. Natl. Acad. Sci. U.S.A. 103*, 16117−16122.

(12) Shinzawa-Itoh, K., Aoyama, H., Muramoto, K., Terada, H., Kurauchi, T., Tadehara, Y., Yamasaki, A., Sugimura, T., Kurono, S., Tsujimoto, K., Mizushima, T., Yamashita, E., Tsukihara, T., and Yoshikawa, S. (2007) Structures and physiological roles of 13 integral lipids of bovine heart cytochrome c oxidase. *EMBO J. 26*, 1713−1725.

(13) Aoyama, H., Muramoto, K., Shinzawa-Itoh, K., Hirata, K., Yamashita, E., Tsukihara, T., Ogura, T., and Yoshikawa, S. (2009) A peroxide bridge between Fe and Cu ions in the O_2 reduction site of fully oxidized cytochrome c oxidase could suppress the proton pump. *Proc. Natl. Acad. Sci. U.S.A. 106*, 2165−2169.

(14) Shimokata, K., Katayama, Y., Murayama, H., Suematsu, M., Tsukihara, T., Muramoto, K., Aoyama, H., Yoshikawa, S., and Shimada, H. (2007) The proton pumping pathway of bovine heart cytochrome c oxidase. *Proc. Natl. Acad. Sci. U.S.A. 104*, 4200−4205.

(15) Ganesan, K., and Gennis, R. B. (2010) Blocking the K-pathway still allows rapid one-electron reduction of the binuclear center during the anaerobic reduction of the aa_3-type cytochrome *c* oxidase from *Rhodobacter sphaeroides*. *Biochim. Biophys. Acta 1797*, 619−624.

(16) Konstantinov, A. A., Siletsky, S., Mitchell, D., Kaulen, A., and Gennis, R. B. (1997) The roles of the two proton input channels in cytochrome c oxidase from *Rhodobacter sphaeroides* probed by the effects of site-directed mutations on time-resolved electrogenic intraprotein proton transfer. *Proc. Natl. Acad. Sci. U.S.A. 94*, 9085−9090.

(17) Brändén, M., Sigurdson, H., Namslauer, A., Gennis, R. B., Ädelroth, P., and Brzezinski, P. (2001) On the role of the K-proton transfer pathway in cytochrome c oxidase. *Proc. Natl. Acad. Sci. U.S.A. 98*, 5013−5018.

(18) Wikström, M., Jasaitis, A., Backgren, C., Puustinen, A., and Verkhovsky, M. I. (2000) The role of the D- and K-pathways of proton transfer in the function of the haem-copper oxidases. *Biochim. Biophys. Acta 1459*, 514−520.

(19) Ädelroth, P., Svensson Ek, M., Mitchell, D. M., Gennis, R. B., and Brzezinski, P. (1997) Glutamate 286 in cytochrome aa_3 from *Rhodobacter sphaeroides* is involved in proton uptake during the reaction of the fully-reduced enzyme with dioxygen. *Biochemistry 36*, 13824−13829.

(20) Brzezinski, P., and Ädelroth, P. (1998) Pathways of proton transfer in cytochrome c oxidase. *J. Bioenerg. Biomembr. 30*, 99−107.

(21) Soulimane, T., Buse, G., Bourenkov, G. P., Bartunik, H. D., Huber, R., and Than, M. E. (2000) Structure and mechanism of the aberrant ba_3-cytochrome *c* oxidase from *Thermus thermophilus*. *EMBO. J. 19*, 1766−1776.

(22) Luna, V. M., Chen, Y., Fee, J. A., and Stout, C. D. (2008) Crystallographic studies of Xe and Kr binding within the large internal cavity of cytochrome ba_3 from *Thermus thermophilus*: Structural analysis and role of oxygen transport channels in the heme-Cu oxidases. *Biochemistry 47*, 4657−4665.
(23) Chang, H. Y., Hemp, J., Chen, Y., Fee, J. A., and Gennis, R. B. (2009) The cytochrome ba_3 oxygen reductase from *Thermus thermophilus* uses a single input channel for proton delivery to the active site and for proton pumping. *Proc. Natl. Acad. Sci. U.S.A. 106*, 16169−16173.
(24) Tiefenbrunn, T., Liu, W., Chen, Y., Katritch, V., Stout, C. D., Fee, J. A., and Cherezov, V. (2011) High resolution structure of the ba_3 cytochrome *c* oxidase from *Thermus thermophilus* in a lipidic environment. *PLoS One 6*, No. e22348.
(25) Koutsoupakis, C., Kolaj-Robin, O., Soulimane, T., and Varotsis, C. (2011) Probing protonation/deprotonation of tyrosine residues in cytochrome ba_3 oxidase from *Thermus thermophilus* by time-resolved step-scan Fourier transform infrared spectroscopy. *J. Biol. Chem. 286*, 30600−30605.
(26) Giuffrè, A., Forte, E., Antonini, G., D'Itri, E., Brunori, M., Soulimane, T., and Buse, G. (1999) Kinetic properties of ba_3 oxidase from *Thermus thermophilus*: Effect of temperature. *Biochemistry 38*, 1057−1065.
(27) Siletskiy, S., Soulimane, T., Azarkina, N., Vygodina, T. V., Buse, G., Kaulen, A., and Konstantinov, A. (1999) Time-resolved generation of a membrane potential by ba_3 cytochrome *c* oxidase from *Thermus thermophilus*. Evidence for reduction-induced opening of the binuclear center. *FEBS Lett. 457*, 98−102.
(28) Smirnova, I. A., Zaslavsky, D., Fee, J. A., Gennis, R. B., and Brzezinski, P. (2008) Electron and proton transfer in the ba_3 oxidase from *Thermus thermophilus*. *J. Bioenerg. Biomembr. 40*, 281−287.
(29) Siletsky, S. A., Belevich, I., Jasaitis, A., Konstantinov, A. A., Wikström, M., Soulimane, T., and Verkhovsky, M. I. (2007) Time-resolved single-turnover of ba_3 oxidase from *Thermus thermophilus*. *Biochim. Biophys. Acta 1767*, 1383−1392.
(30) Smirnova, I., Reimann, J., Von Ballmoos, C., Chang, H. Y., Gennis, R. B., Fee, J. A., Brzezinski, P., and Ädelroth, P. (2010) Functional role of Thr-312 and Thr-315 in the proton-transfer pathway in ba_3 cytochrome *c* oxidase from *Thermus thermophilus*. *Biochemistry 49*, 7033−7039.
(31) Von Ballmoos, C., Gennis, R. B., Ädelroth, P., and Brzezinski, P. (2011) Kinetic design of the respiratory oxidases. *Proc. Natl. Acad. Sci. U.S.A. 108*, 11057−11062.
(32) Einarsdóttir, Ó., Funatogawa, C., Soulimane, T., and Szundi, I. (2012) Kinetic studies of the reactions of O_2 and NO with reduced *Thermus thermophilus* ba_3 and bovine aa_3 using photolabile carriers. *Biochim. Biophys. Acta 1817*, 672−679.
(33) Szundi, I., Funatogawa, C., Fee, J. A., Soulimane, T., and Einarsdóttir, Ó. (2010) CO impedes superfast O_2 binding in ba_3 cytochrome oxidase from *Thermus thermophilus*. *Proc. Natl. Acad. Sci. U.S.A. 107*, 21010−21015.
(34) Kannt, A., Soulimane, T., Buse, G., Becker, A., Bamberg, E., and Michel, H. (1998) Electrical current generation and proton pumping catalyzed by the ba3-type cytochrome c oxidase from *Thermus thermophilus*. *FEBS Lett. 434*, 17−22.
(35) Han, H., Hemp, J., Pace, L. A., Ouyang, H., Ganesan, K., Roh, J. H., Daldal, F., Blanke, S. R., and Gennis, R. B. (2011) Adaptation of aerobic respiration to low O_2 environments. *Proc. Natl. Acad. Sci. U.S.A. 108*, 14109−14114.
(36) Popovic, D. M., and Stuchebrukhov, A. A. (2004) Proton pumping mechanism and catalytic cycle of cytochrome c oxidase: Coulomb pump model with kinetic gating. *FEBS Lett. 566*, 126−130.
(37) Liu, B., Zhang, Y., Sage, J. T., Soltis, S. M., Doukov, T., Chen, Y., Stout, C. D., and Fee, J. A. (2012) Structural changes that occur upon photolysis of the Fe(II) a3-CO complex in the cytochrome ba_3-oxidase of *Thermus thermophilus*: A combined X-ray crystallographic and infrared spectral study demonstrates CO binding to Cu_B. *Biochim. Biophys. Acta 1817*, 658−665.
(38) Woodruff, W. H. (1993) Coordination dynamics of heme-copper oxidases. The ligand shuttle and the control and coupling of electron transfer and proton translocation. *J. Bioenerg. Biomembr. 25*, 177−188.
(39) Koutsoupakis, K., Stavrakis, S., Pinakoulaki, E., Soulimane, T., and Varotsis, C. (2002) Observation of the equilibrium Cu_B-CO complex and functional implications of the transient heme a_3 propionates in cytochrome ba_3-CO from *Thermus thermophilus*. Fourier transform infrared (FTIR) and time-resolved step-scan FTIR studies. *J. Biol. Chem. 277*, 32860−32866.
(40) von Ballmoos, C., Ädelroth, P., Gennis, R. B., and Brzezinski, P. (2012) Proton transfer in ba_3 cytochrome *c* oxidase from *Thermus thermophilus*. *Biochim. Biophys. Acta 1817*, 650−657.
(41) Morgan, J. E., Verkhovsky, M. I., and Wikström, M. (1996) Observation and assignment of peroxy and ferryl intermediates in the reduction of dioxygen to water by cytochrome c oxidase. *Biochemistry 35*, 12235−12240.
(42) Wikström, M., and Morgan, J. E. (1992) The Dioxygen Cycle: Spectral, Kinetic, and Thermodynamic Characteristics of Ferryl and Peroxy Intermediates Observed by Reversal of the Cytochrome-Oxidase Reaction. *J. Biol. Chem. 267*, 10266−10273.
(43) Karpefors, M., Ädelroth, P., Namslauer, A., Zhen, Y. J., and Brzezinski, P. (2000) Formation of the "peroxy" intermediate in cytochrome c oxidase is associated with internal proton/hydrogen transfer. *Biochemistry 39*, 14664−14669.
(44) Faxén, K., Gilderson, G., Ädelroth, P., and Brzezinski, P. (2005) A mechanistic principle for proton pumping by cytochrome c oxidase. *Nature 437*, 286−289.
(45) Verkhovsky, M. I., Morgan, J. E., Verkhovskaya, M. L., and Wikström, M. (1997) Translocation of electrical charge during a single turnover of cytochrome-c oxidase. *Biochim. Biophys. Acta 1318*, 6−10.
(46) Malmström, B. G. (1985) Hypothesis. Cytochrome c oxidase as a proton pump. A transition-state mechanism. *Biochim. Biophys. Acta 811*, 1−12.
(47) Hallén, S., and Nilsson, T. (1992) Proton transfer during the reaction between fully reduced cytochrome c oxidase and dioxygen: pH and deuterium isotope effects. *Biochemistry 31*, 11853−11859.
(48) Ädelroth, P., Ek, M., and Brzezinski, P. (1998) Factors Determining Electron-Transfer Rates in Cytochrome *c* Oxidase: Investigation of the Oxygen Reaction in the *R. sphaeroid*es and Bovine Enzymes. *Biochim. Biophys. Acta 1367*, 107−117.
(49) Namslauer, A., Aagaard, A., Katsonouri, A., and Brzezinski, P. (2003) Intramolecular proton-transfer reactions in a membrane-bound proton pump: The effect of pH on the peroxy to ferryl transition in cytochrome c oxidase. *Biochemsitry 42*, 1488−1498.
(50) Brzezinski, P., and Johansson, A. L. (2010) Variable proton-pumping stoichiometry in structural variants of cytochrome c oxidase. *Biochim. Biophys. Acta 1797*, 710−723.
(51) Chakrabarty, S., Namslauer, I., Brzezinski, P., and Warshel, A. (2011) Exploration of the cytochrome c oxidase pathway puzzle and examination of the origin of elusive mutational effects. *Biochim. Biophys. Acta 1807*, 413−426.
(52) Babcock, G. T., and Wikström, M. (1992) Oxygen activation and the conservation of energy in cell respiration. *Nature 356*, 301−309.
(53) Salomonsson, L., Faxén, K., Ädelroth, P., and Brzezinski, P. (2005) The timing of proton migration in membrane-reconstituted cytochrome c oxidase. *Proc. Natl. Acad. Sci. U.S.A. 102*, 17624−17629.
(54) Belevich, I., Bloch, D. A., Belevich, N., Wikström, M., and Verkhovsky, M. I. (2007) Exploring the proton pump mechanism of cytochrome c oxidase in real time. *Proc. Natl. Acad. Sci. U.S.A. 104*, 2685−2690.
(55) Lepp, H., and Brzezinski, P. (2009) Internal charge transfer in cytochrome c oxidase at a limited proton supply: Proton pumping ceases at high pH. *Biochim. Biophys. Acta 1790*, 552−557.